

Observation of Three Characteristic Energy Scales (Energy Gaps) in the Conductance of Underdoped $\text{YBa}_2\text{Cu}_3\text{O}_{6+x}$ Junctions

G. Koren, N. Levy and E. Polturak

Department of Physics, Technion-Israel Institute of Technology, Haifa, 32000, ISRAEL

Conductance measurements in underdoped $\text{YBa}_2\text{Cu}_3\text{O}_{6+x}$ (YBCO) tunneling junctions in the $a-b$ plane are reported which reveal that in addition to the dominant $d_{x^2-y^2}$ -wave component of the order parameter (OP), a small is (or id_{xy}) component is also present, and both overlay a broad pseudogap feature. Extensive measurements by other groups from Urbana, Tel-Aviv and Jerusalem in optimally or overdoped YBCO films showed a splitting of the zero bias peak. This was interpreted as due to the existence of a small imaginary component in the OP of YBCO. We show that also in underdoped YBCO there is an additional small is component in the OP. In ramp type (edge) junctions, oriented along different directions in the $a-b$ plane, we find that the $d_{x^2-y^2}$ -wave gap is suppressed in the region near the node, but has a non zero value of $\Delta = 3.0 \pm 0.5$ mV at the node itself. This result supports the existence of a sub-dominant is component in the order parameter of underdoped YBCO.

PACS numbers: 74.20.Rp, 74.50.+r, 74.72.Bk.

1. INTRODUCTION

The pairing symmetry in the cuprate superconductors has been discussed in detail by Tsuei and Kirtley a couple of years ago in a comprehensive review article.¹ The consensus was that the order parameter in the high temperature superconductors (HTSC) has a dominant $d_{x^2-y^2}$ wave symmetry, and this was demonstrated in many experiments.¹⁻⁴ These include phase-sensitive studies in corner, edge and tricrystal junctions,^{1,2} and directional

G. Koren, N. Levy, and E. Polturak

tunneling in the a - b plane which show a gap structure along the main axes and a zero bias peak (ZBP) along the node.³⁻⁵ Other experiments however, show a splitting of the ZBP,⁵⁻⁷ and this is interpreted as due to the existence of a sub-dominant is or id_{xy} component in the order parameter of the HTSC. This component is responsible for the observation of spontaneous magnetization which was found during the transition to superconductivity of the HTSC samples.⁸ While the phase-sensitive experiments did prove that the order parameter changes sign as $\cos(2\theta)$, where θ is the in-plane angle, the exact angular dependence of the energy gap was not determined until recently when detailed tunneling experiments in YBCO were performed.⁹ In BSCO 2212 though, angle resolved photo-emission (ARPES) measurements yielded the full angular dependence of the order parameter which in one case followed a clean $d_{x^2-y^2}$ wave symmetry,¹⁰ while in another case, deviated from it with an extended node region.¹¹ Also, c -axis grain boundary junctions were produced in BSCO single crystals at different coupling angles, and the critical current I_c was measured.¹² Here however, the anisotropy seems to reflect defects in the boundary (exponential decay of I_c versus the mismatch angle) more than the symmetry of the order parameter. In the present study we used tunneling in $\text{YBa}_2\text{Cu}_3\text{O}_{6+x}$ (YBCO) based ramp type (or edge) junctions, to measure the full angular dependence of the conductance spectra. We extended our previous results where we found a modified $d_{x^2-y^2}$ wave gap behavior with extended node region and a non zero gap at the node,⁹ by a systematic study of the temperature and magnetic field dependence of our spectra. We find three distinct energy scales in the conductance spectra, which can be distinguished under different fields and temperatures. These are the two superconducting $d_{x^2-y^2}$ and is (or id_{xy}) energy gaps, and the pseudogap.

2. EXPERIMENTAL

Underdoped YBCO based ramp type junctions with Fe doped YBCO barriers were prepared by a multi-step process. The epitaxial thin film layers were prepared by laser ablation deposition, and patterning was done by waterless deep UV photolithography using PMMA resists, and etching by Ar ion milling.¹³ We used the same $\text{YBa}_2\text{Fe}_{0.45}\text{Cu}_{2.55}\text{O}_{6+x}$ (YBFeCO) barrier as before,¹³ but patterned the 10 junctions on the (100) SrTiO_3 wafer each in a different direction (θ) in the a - b plane of the films. It is important to note that three separate milling steps of the base electrode were used, each time patterning only one group of junctions within a spread of $\pm 15^\circ$ while protecting the others with a copper shadow mask. This was

Observation of Three Energy Gaps in YBCO

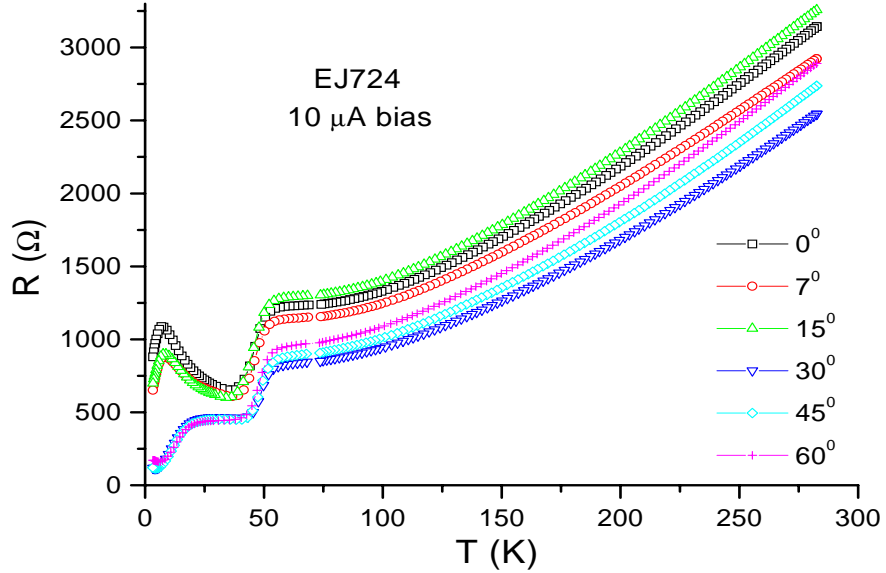


Fig. 1. Resistance versus temperature of 6 of the 10 junctions on the wafer.

done in order to obtain quite similar ramp angles of $\sim 35 \pm 5^\circ$ in all the 10 junctions on the wafer. The thickness of the base and cover electrodes was 90 nm, while the barrier thickness was 22 nm. The width of each ramp type junction was $5 \mu\text{m}$. A gold layer was deposited on top of the cover electrode and patterned to produce the 4×10 contact pads for the 4-probe transport measurements. Atomic force microscope (AFM) images of the exposed ramp of the YBCO base electrode in our junctions show that the ramp morphology is quite uniform laterally and rough on a scale of less than one unit cell height ($< 1\text{nm}$).⁹ This indicates that the interface in our junctions is smooth on the same scale which is smaller than a coherence length ξ , and has a well defined crystallographic orientation. Thus, our angular dependent results are hardly affected by micro-faceting and averaging over this small interface roughness.

3. RESULTS

Fig. 1 shows the resistance versus temperature of 6 of the 10 junctions on a wafer. Compared to our previous study⁹ slightly less oxygen was used in the annealing process resulting in more resistive junctions ($\times 5$) and underdoped YBCO electrodes which become superconducting at 50K.¹³ For junctions close to the main axis orientation, the resistance goes through a

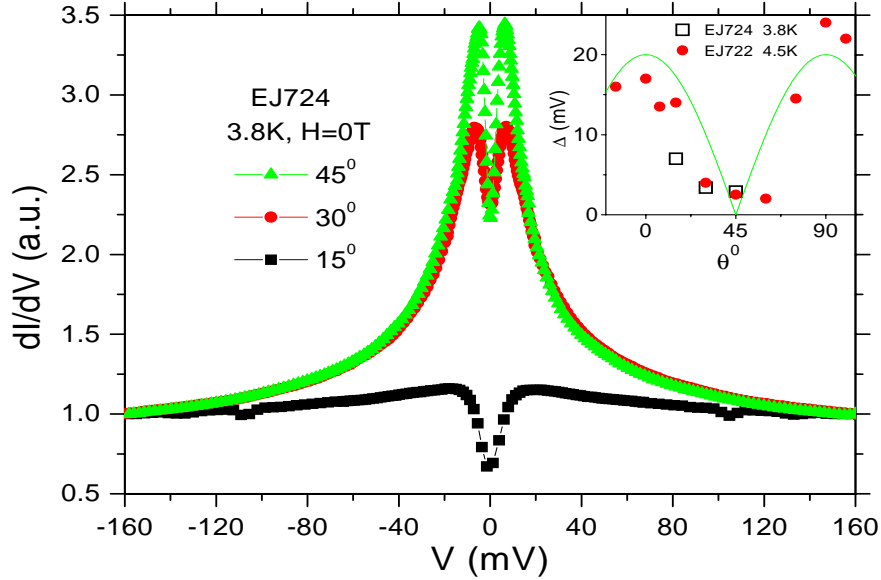


Fig. 2. Normalized conductance spectra of the 15° , 30° and 45° junctions. The inset shows the energy gap versus angle (open squares), and also includes data from Ref. 9 (solid circles).

minimum at 40K, increases to a local maximum at 10K and then decreases at lower temperature. For junctions with orientations near the node orientation (30° and 45°) and the one near the main axis (15°). For the sake of simplicity, we take the measured tunneling gap Δ of our SIS junctions as the peak to peak voltage difference divided by 4. The resulting $\Delta(\theta)$ is shown in the inset of Fig. 2 together with the gaps measured in our previous study⁹ and $\Delta_0|\cos(2\theta)|$ where $\Delta_0 = 20$ mV. Both sets of data agree quite well, and the dominant $d_{x^2-y^2}$ -wave symmetry is clearly seen. The finite gap value at $\theta = 45^\circ$ is well reproduced, and equals to 3 ± 0.5 mV which clearly overlaps the 2.5 ± 0.3 mV value found before. This gap is not expected for a pure $d_{x^2-y^2}$ -wave superconductor, and therefore seems to imply the existence of an additional sub-dominant component to the order parameter. Possible

Fig. 2 shows the measured conductance normalized to the high bias values of 3 of the 10 junctions on the wafer. Like in our previous study,⁹ we find a different angular dependence for the junctions near the node orientation (30° and 45°) and the one near the main axis (15°). For the sake of simplicity, we take the measured tunneling gap Δ of our SIS junctions as the peak to peak voltage difference divided by 4. The resulting $\Delta(\theta)$ is shown in the inset of Fig. 2 together with the gaps measured in our previous study⁹ and $\Delta_0|\cos(2\theta)|$ where $\Delta_0 = 20$ mV. Both sets of data agree quite well, and the dominant $d_{x^2-y^2}$ -wave symmetry is clearly seen. The finite gap value at $\theta = 45^\circ$ is well reproduced, and equals to 3 ± 0.5 mV which clearly overlaps the 2.5 ± 0.3 mV value found before. This gap is not expected for a pure $d_{x^2-y^2}$ -wave superconductor, and therefore seems to imply the existence of an additional sub-dominant component to the order parameter. Possible

Observation of Three Energy Gaps in YBCO

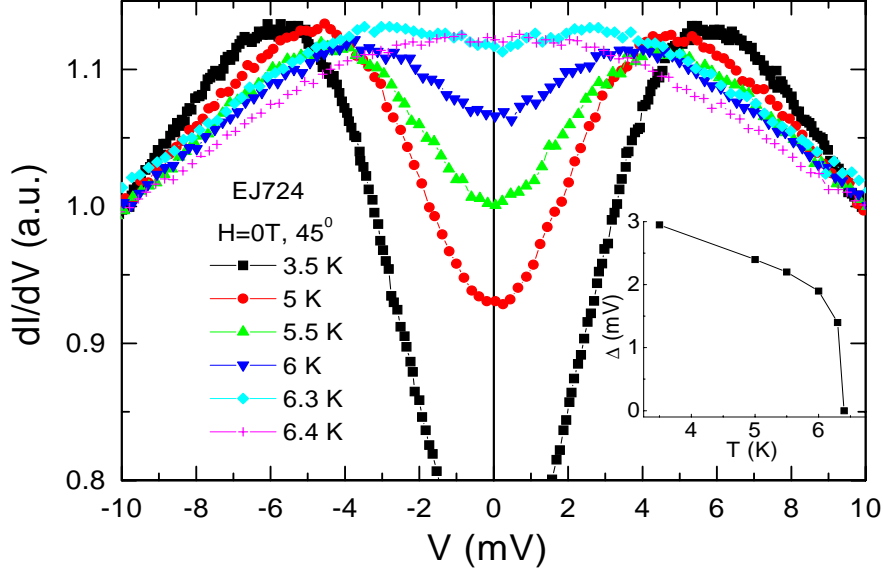


Fig. 3. Normalized conductance spectra of the 45° junction at several temperatures. The inset shows the energy gap versus temperature.

candidates for this component are the s , is or id_{xy} symmetries. A subdominant s symmetry should be ruled out since it still has real nodes (zeroes of the OP) and should produce only a zero bias peak near the 45° orientation but not a small gap-like feature as observed here. Since there is evidence for a pair potential component with a broken time reversal symmetry that gives rise to a splitting of the zero bias peak in the conductivity,^{6,7} the is -wave scenario is more likely. An id_{xy} -wave scenario was invoked by Carmi *et al.* to explain their spontaneous magnetization results,⁸ but calculations using this scenario do *not* yield a gap-like feature at low bias at the node itself.¹⁵ A tunneling cone of $\pm 15^\circ$ however, does yield a small gap structure in this case, and thus the id_{xy} -wave scenario is still possible.

Fig. 3 shows conductance spectra of the 45° junction for various temperatures, together with the gap values $\Delta(T)$ inferred from the peak to peak distances. Up to about 6K the gap values are almost temperature independent, while at higher temperatures, the gap fills up and decreases with temperature. This is similar but not identical to our previous finding where the gap persisted up to 12K, and the decrease with increasing temperature was slower. The differences may be due to the higher R_N values in the present study (about $\times 5$), and the lack of interfering effects of geometrical resonances that appeared in our previous investigations.^{9,14} Here again, the

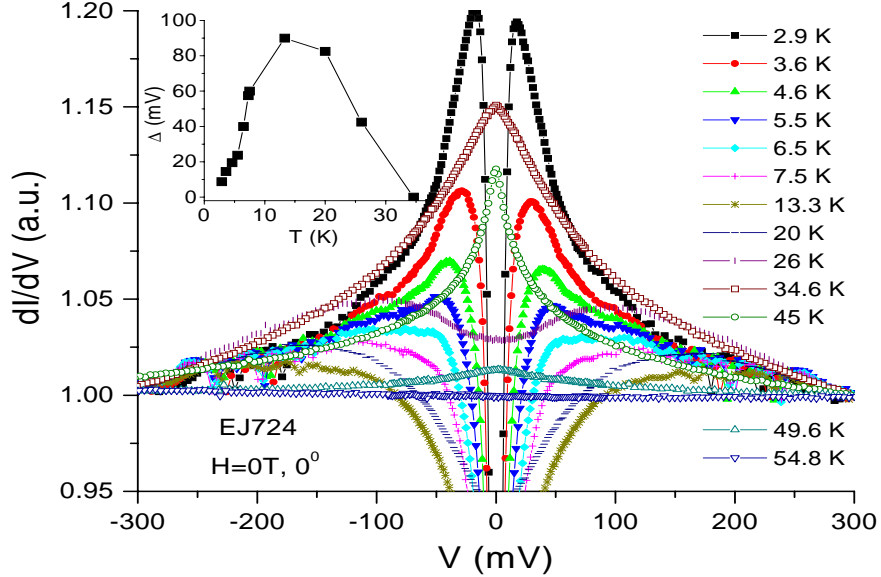


Fig. 4. Normalized conductance spectra of the 0° junction for various temperatures (main panel), and the energy gap versus temperature (inset).

tunneling conductance curve crosses over at 7K to a zero bias peak behavior with increasing temperature, while the junction resistance is almost constant in this temperature range. The results of Fig. 3 lend further support to the interpretation of the observed peaks in Fig. 2 in the vicinity of the node as due to real gap structures.

Fig. 4 presents conductance spectra of the 0° junction at many temperatures. As summarized in the inset, these spectra reveal significant changes in the energy gap values versus temperature. At low temperatures up to 6K we see gaps of about 10-20 mV, which reflect the $is + d_{x^2-y^2}$ symmetries. At temperatures of 6.5-7.5K, there is a sharp transition to much larger gaps which reach apparent values of around 80-90 mV at 10-20K, and then decay to zero at about 30K. At a first glance, these large gaps can be attributed to the pseudogap, but the fact that we observe a strong and broad Andreev like peak in the conductance at higher temperatures of 35-45K complicates this picture. It is possible that the broad gaps result from a combination of the suppressed $is + d_{x^2-y^2}$ gaps and the broad Andreev like enhancement peak. Support to this scenario results from the observation that the 45K peak is narrower than the 34.6K spectra, which means that the former still contains a significant gap contribution. At 54.8K the conductance spectrum is totally flat. This however, does not indicate the absence of a pseudogap,

Observation of Three Energy Gaps in YBCO

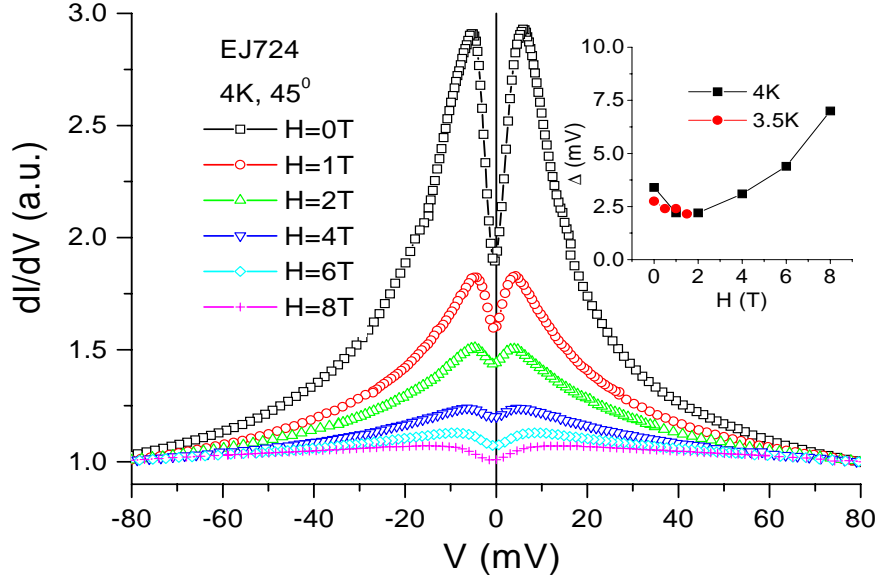


Fig. 5. Normalized conductance of the 45° junction at several magnetic fields. The inset presents the energy gap versus field, and includes low field data from another measurement on the same junction.

but only reflects the fact that the YBCO electrodes become normal at this temperature, and that we measure mostly the voltage drop across the electrodes and not the junction. Another factor that should be taken into consideration is possible heating of the junction and its near vicinity at the high voltages used in Fig. 4. This could lead to the decreased conductance with increasing voltage, and the broad conductance peaks above 34K can be due heating effects and not to Andreev processes. The conductance spectra under magnetic fields which will be discussed next, will help us to elucidate these unresolved questions.

Fig. 5 shows the conductance spectra of the 45° junction at 4K in few magnetic fields normal to the wafer, together with the corresponding *is* gap values versus field. We find a small gap suppression at low fields, and then a significant increase with increasing field ($\times 3$ for 8T). We note first that this data represents a huge change of conductance between low and high bias voltages compared to that of Fig. 4 (200% versus 10% for the 4K and $H=0T$ data). Moreover, the bias voltages in Fig. 5 are smaller than in Fig. 4, and all the gap values are smaller than 10 mV, which is beneficial towards reducing possible heating effects. The present results are reminiscent of the ZBP splitting spectra reported before where the splitting increases with field

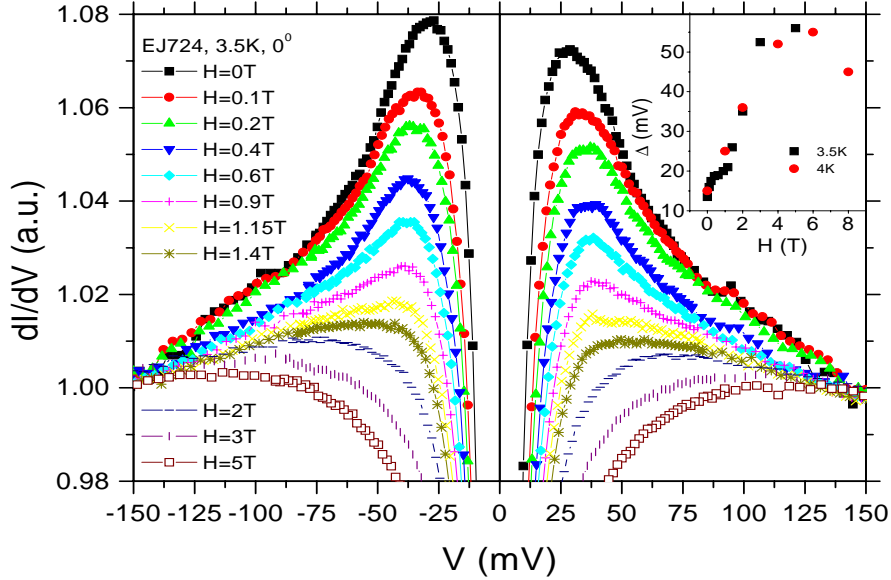


Fig. 6. Normalized conductance spectra of the 0° junction at several magnetic fields. The inset shows the energy gap behavior versus field (squares), including data of the same junction whose spectra are not shown on the main panel (circles).

but with smaller gap values.^{6,7} Clearly, the whole spectrum is suppressed with field, but since it overlays a broad and shallow Andreev like peak, the suppression leads to opening of the gap with increasing field. It is quite likely that the gap seen at 8T is the pseudogap, and in this case there are hardly any heating effects to mask it.

Fig. 6 shows the conductance spectra of the 0° junction at 3.5K at several magnetic fields normal to the wafer, together with the corresponding gap values versus field. Increasing the field seems to play a similar role to the increase of temperature as seen in Fig. 4. With increasing field, the $is + d_{x^2-y^2}$ gap increases from 13 to 20 mV up to 1.5T (due to the suppression of the is gap) with a plateau at 18 mV. Then it crosses over at 2-3T to the pseudogap at 55 mV in the 4-6T range, and decreases again at 8T. Due to the lower bias voltages, and better superconducting properties of the YBCO electrodes at the lower temperature, there are less heating effects here. So we have better reason to believe that we actually measure the pseudogap, and not a heating artifact. We can now state that a comparison of the 8T gaps at 45° (Fig. 5) and 0° (Fig. 6) yields an angular dependence of the pseudogap, which has not been measured before.

Observation of Three Energy Gaps in YBCO

Finally, since our results are obtained in underdoped YBCO junctions with Fe doped YBCO barrier, it is possible that magnetic scattering at the barrier plays a role in the measured conductance.¹⁶ To check this, we are currently studying ramp type junctions with a non magnetic Ga doped YBCO barrier. Preliminary results show the existence of a small *is* gap at the 45° junctions like we find in the present study and disappearance of this gap between 10 and 15K, but we do not yet have data under magnetic fields. Thus, magnetic scattering in the barrier of our junctions is probably *not* the origin of the features reported here, but this conclusion needs further systematic testing in the junctions with Ga doped YBCO barriers.

In conclusion, our results demonstrate the existence of a modified $d_{x^2-y^2}$ -wave order parameter in underdoped YBCO, with extended node regions, and a sub-dominant *is* (or id_{xy}) component whose value is about 2.5-3 mV. Both of these *superconducting* gaps in the conductance spectra overlay a broad and shallow pseudogap feature which is *non superconducting* and has an angular dependence. Thus in all, we observe in the present study three different energy scales (or gaps) in the conductance of underdoped YBCO.

ACKNOWLEDGMENTS

We are grateful to L. Shkedy, O. Millo and G. Deutscher for useful discussions. This research was supported in part by the Israel Science Foundation, the Heinrich Hertz Minerva Center for HTSC, and by the Fund for the Promotion of Research at the Technion.

REFERENCES

1. C. C. Tsuei and J. R. Kirtley, *Rev. Mod. Phys.* **72**, 969 (2000) and references therein.
2. D. A. Wollman, D. J. Van Harlingen, J. Giapintzakis and D. M. Ginsberg, *Phys. Rev. Lett.* **74**, 797 (1995).
3. J. Y. T. Wei, N. C. Yeh, D. F. Garrigus and M. Strasik, *Phys. Rev. Lett.* **81**, 2542 (1998).
4. O. Neshet and G. Koren, *Phys. Rev. B* **60**, 14869 (1999).
5. A. Sharoni, G. Koren and O. Millo, *Europhys. Lett.* **54**, 675 (2001).
6. M. Covington, M. Aprili, E. Paraoanu, L. H. Greene, F. Xu, J. Zhu and C. A. Mirkin, *Phys. Rev. Lett.* **79**, 277 (1997).
7. R. Krupke and G. Deutscher, *Phys. Rev. Lett.* **86**, 4634 (1999).

G. Koren, N. Levy, and E. Polturak

8. R. Carmi, E. Polturak, G. Koren and A. Auerbach, *Nature* **404**, 853 (2000).
9. G. Koren and N. Levy, *Europhys. Lett.* **59**, 121 (2002). Note that in Fig. 1 of this paper the scales are in nm.
10. H. Ding *et al.*, *Phys. Rev. B* **54**, R9678 (1996).
11. H. Ding, M. R. Norman, T. Mochiku, K. Kadowaki and J. Giapinzakis, *Nature* **382**, 51 (1996).
12. Y. Takano *et al.*, *Phys. Rev. B* **65**, 140513(R) (2002).
13. O. Neshar and G. Koren, *Appl. Phys. Lett.* **74**, 3392 (1999).
14. O. Neshar and G. Koren, *Phys. Rev. B* **60**, 9287 (1999).
15. Y. Tanaka and S. Kashiwaya, *Phys. Rev. B* **53**, 9371 (1996).
16. L. Y. L. Shen and J. M. Rowell, *Phys. Rev.* **165**, 566 (1968).